Modeling and Simulation of a Large-Scale Grid-Connected Wind-Turbine-PV-Battery-Diesel Hybrid Power System.

Osama Alagili1, Faculty of Engineering and Applied Science, Memorial University of Newfoundland, St. John's NL, A1B 3X5 Canada.

ABSTRACT

This research aims to investigate and analyze PV generators, wind energy generators, and energy storage system for stabilizing and grid support functions. The analysis will proceed from both an economic and a technological perspective. More specifically, we will look at the blueprints for a 10 MW solar power facility in the eastern Canadian province of Prince Edward Island (PE). Our investigation will include estimating the facility's annual performance and formulating the performance ratio against various types disturbances. This model incorporates work that is already being done on wind turbines (WEICan) in PE, and the WEICan data is combined with the model to produce a 20 MW simulation using a BESS (battery energy storage system) to create a novel grid-connected photovoltaic wind turbine BESS diesel generator (or PV-WT-BESS-DG) hybrid system that also includes controllers and converters. A perturb and observe (P&O) algorithm is employed to optimize the amount of energy produced according to the maximum power point tracker (MPPT) and the proposed model undergoes simulated tests for a variety of weather- and solar-dependent operating conditions.

Introduction.

The recent increase in global demand for energy has opened the door to new types of resources to supplement or even replace traditional petroleum-based energy production. Researchers and the energy industry are particularly interested in resources and approaches which are considered "green" and environmentally friendly, especially renewable options. One such energy approach involves micro grid technology. Micro grids can be loosely defined as energy systems which are used to balance distributed energy resources. They employ various types of energy management for hybrid energy production systems, aiming to achieve the best resource distribution schedule under ever-changing weather conditions. Photovoltaic (PV) wind turbine systems that are grid-connected are proving to be strong contenders for the title of best renewable energy format for large-scale production. A closer investigation into the performance of these systems could lead to better next-generation grid-connected systems, especially with regard to general maintenance and operation. Micro grids are distributed energy resources (DER) that function as either grid-connected or islanded systems, the most common of which are energy storage systems (ESS) or renewable energy sources (RES). As a means to standardize microgrid control, the hierarchical operational approach is generally used. Alternative energy sources are gaining in popularity as a result of restrictions on the use of fossil fuels as well as a general turning away from other traditional fuel types such as nuclear sources. One energy source that is moving to the forefront

of alternative energy options is photovoltaic (PV) panels or modules. PVs, which use semiconductors to change sunlight to electricity, have been shown to be not only environmentally friendly but also reliable and relatively low maintenance. Solar PV systems can exhibit a broad range of performance success depending on the environmental conditions under which they operate [1]. Some recent studies give examples of typical operational conditions. Modeled a 5M, WSPV power plant that was intended to provide electricity for dozens of cities in Iran [2]. By applying RET scree software, the researchers discovered major differences among the cities with regard to operational performance, in that, for instance, the city of Bushier showed the greatest capacity factor (26%) while the city of Anzali showed the lowest (16%), with 22% being the overall average capacity factor [2]. In another study, analyzed a 3.6 kW grid-connected solar PV system installed on an Egyptian rooftop [3]. The power produced contributed to a 220 V, 50 Hz low-voltage grid, with the researchers monitoring usage for over a year. Additional investigations were carried out by Shiva et al. That tested the validity of using solar PV modules to produce energy for 10 MW PV power plants in India. The researchers found that CdTe solar modules produced the greatest energy for their purposes [4]. Along with solar energy alternatives, wind energy has also been growing in usage and popularity. In fact, wind power installations have expanded exponentially, increasing installed capacity to 318 GW in 2013 from just 39 GW in 2003 [5]. By 2014, wind power was contributing 4% to overall power generation globally [6]. However, solar power faces unique challenges (i.e., lack of sunlight affects reliability), similarly wind power also has its own issues, the main one being that wind speeds are generally inconsistent. This inconsistency can cause power installations to fall short of satisfying consumption demand [7]. To resolve the problem of power fluctuations caused by wind inconsistency, researchers are looking to energy storage as a solution .In this approach [8], a supervisory control and data acquisition (SCADA) system is used to record high quality data from existing wind facility components, which will then be analyzed and applied to future operations. In instances where energy is not being produced due to lack of sufficient wind, the BESS (battery energy storage system) can be used although costs are still very high. Some areas have developed a rate-paying structure specifically geared towards commercial users that involves both a demand charge (e.g., the highest average 30-minute cost) for billing periods in addition to an energy charge. However, a better approach would be to lower both the demand and energy charges through changes to the BESS charge, i.e., applying it only when the wind farm produces enough power to warrant it. Researchers in [9] have further investigated how wind farms can utilize storage systems to deal with the issue of energy-production inconsistencies due to fluctuations in wind speed. The research points to two specific solutions: battery storage systems that can be implemented for long-term fluctuations, and capacitors that can be used to offset short-term ones. In [10], researchers applied various control strategies that involved a vanadium flow battery, while in [11] a sodium–nickel chloride battery was tested. A study in [12] employed a 25MWh/100MW NaS battery as the main regulator for back-stopping wind power for a modeled scenario where a whole wind farm (100MW) is knocked out of service. Another study looked for ways to offset fluctuations in wind energy while at the same time improve battery life. In that work, the researchers applied a power reference that was formulated according to a one-hour wind power average. However, the study results showed negligible benefits, as the wind power average could only be calculated after the hour was expired, which meant that the net power rate stayed the same and did not lower battery usage [13]. Additional research investigated the use of lithium batteries (at 400 kW/744 kW h per unit)

and a wind turbine (at 800 kW) in a system on a First Nations reserve in western Canada [14]. The results indicated an improvement in output fluctuations of up to 65% and showed that the approach was able to offer dispatch power for high-load phases. Furthermore, the system was able to restrict the battery from charging off the grid in times of reduced or calm winds [14]. Other recent research [15] looked at using energy storage towards regulating frequencies on wind farms, while a study based in China [16] investigated wind farm control strategies in relation to spillage requirements in a 5 MW x 2 h BESS. That research primarily looked at distribution generation and grid optimization via a PV/WT/battery hybrid system. Indeed, hybrid systems have been increasing in popularity in the past few decades. In China, [17] studied hybrid wind-solar systems that use banks of batteries as a means to formulate the best configurations. In Iraq, [18] developed a different kind of hybrid wind-solar system for producing energy in grid-connected systems across three cities. In Minnesota, USA, [19] developed a model for a hybrid wind-solar energy facility that applied data from wind speed and solar irradiation, while in Turkey, [20] studied optimal sizing for wind/PV hybrid systems. As well, a number of research models have been developed for PV/WT power systems. Kim [21] devised a grid-connected PV model by employing PSCAD/EMTDC electromagnetic transient analysis. MATLAB/SIMULINK software enabled. Tsai [22] to design and test an insulated PV model, while Adriana [23] created a PV model for simulation platforms like CPLEX. In [24], Khan outlined details for wind-fueled cell hybrid and integrated energy systems, and in [25], Chayawatto presented his model for an AC/DC full-bridge switching converter that included current control of a PV grid-connected system. This study specifically investigated systems under the islanding phenomenon, where a grid system disconnects but distributed power is still supplied to local loads. Finally, in [26], Lihui presented a prospective hybrid wind power/solar photovoltaic power/ and pumped storage power geared to grid-independent users. The present research work, while acknowledging the contributions of previous studies, develops and provides a performance estimation for a large-scale grid-connected solar energy-producing facility that can integrate with the PEI wind R&D facility and generate 20 MW. The performance estimation for a 10 MW grid-connected solar PV energy-producing facility aims to achieve two specific objectives:

(1) Use PVSYST software to size the proposed system by estimating a variety of yearly yields (energy, array and reference) as well as potential system losses.

(2) Compare data derived from PVSYST and MATLAB/SIMULINK software with data on performance for the proposed large-scale grid-connected PV/WT/battery/diesel hybrid energy-producing system. The validity of the proposed system is tested through simulations performed on the dynamic model [4] [27] [28].

SYSTEM DESCRIPTION AND MODELING.

A. Solar PV-grid.

1. Description of the system.

Typical grid-connected solar PV systems are comprised of grid-connecting components, power-conditioners, and solar panels. Under favorable conditions, grid-connected solar PV systems contribute excess energy to utility grids. However, this process differs for standalone systems, where batteries must be employed for excess power storage.

1.1 Project site location.

The site of the proposed project is 46.25° N and 63.13° W, at near sea level

1.2 Solar panel details.

A 10 MW solar PV energy-producing facility is proposed for the site using Cadmium Telluride (CdTe) PVs. The power produced in the regional grid is mainly from fossil fuels, but the solar PV-fueled plant is anticipated to reduce GHG emissions while exporting to the primary grid. The proposed solar PV facility comprises eight separate sections of 1.25 MWp, along with double 630 kW inverters, which are used to change the PV modules' DC energy to AC energy. To optimize the amount of solar irradiation hitting the panels, all of the PV modules are positioned in a south-facing alignment at a 47^{o} angle [29].

The following three charts provide additional details on the facility and its components.

Parameter	Value
PV module	FS – 380
PV module peak power (Wp)	80
Modules per plant	125,025
Modules per plot	15,600
Strings per plot	1,040
Inverters	SMA SC 630CP
Inverter power (kVA)	630 kW
Inverters per plot	2
Total plots	8
Total inverters	16
Mounting structure	Haticon (German make)

PV module specifications:

Type	Thin Film Cadmium Telluride (CdTe)
Max. Output at STC (W), Pmax	80
Maximum Power Voltage, Vmpp (Volts)	50.7
Maximum Power Current, Impp (A)	1.58
Open-circuit voltage, VOC (V)	61.7
Short-circuit current, ISC (A)	1.76
Length (mm)	1200
Width (mm)	600
Thickness (mm)	6.8
Weight (kg)	12

Inverter specifications:

Inverter	SMA Sunny Central 630CP
Max. DC voltage	1000 V
PV voltage range, MPPT	500 - 820 V
Max. Input current	1350
Number of MPP trackers	1
Max. Number of strings (parallel)	9

Nominal AC output	630 kVA
Max. Output current	1271 A
Nominal AC voltage/range	315 V ± 10%
AC grid frequency	60 Hz
Max. efficiency	0.987
Euro ETA	0.985
Normal ambient temperature range	-20 ^{o}C - +50 ^{o}C
Operation temperature range	-20 ^{o}C - +50 ^{o}C
Consumption: operating (standby)/night	<1500 W/ 100W
Warranty	5 years

The energy-producing output capacity is estimated at maximum 10 MWp, with the aggregate capacity measuring 10.02 MW [29].

1.3 Panel tilt.

The PV array tilt (47°) reflects both the geographical location of the site and its latitude and has been developed to absorb the maximum amount of solar radiation and thus extract the most energy output [30].

2. Solar PV system performance analysis.

PVSYST software is used for estimating the grid-connected solar PV energy facility, applying performance parameters (e.g., power generation, system losses and solar resources) from the International Energy Agency (IEA) [31]. Other parameters to be estimated and tested include system and reference yield and performance ratio [29].

2.1 Parameters applied in the present study.

Array yield.

The array yield is defined as being the time that is equal to PV plant operation under solar generator power PO enough for producing array DC power Ea as (kW h/d∗kWp) units.

$Y_A = EA/PO$

where array energy output per day is EA = Idc∗Vdc∗t (kW h); hence:

I_{dc} = DC current (A)

V_{dc} = DC voltage (V)

P_O = nominal power at standard test conditions (STC).

Reference yield.

This refers to the power produced under ideal circumstances and is defined as total in-plane irradiance H sub-divided by reference irradiance G from a PV source. Where G equates to 1 kW/m^2, Yr represents peak sun hours (in numeric expression) as units of solar radiation for kW h/m^2. In other words, Yr indicates a PV system's solar radiation. Reference yield is given in h/d units and is derived from factors such as PV array orientation, standard weather conditions, and geographical location.

Y_R = [kW h/m^2]/1 kW/m^2.

$Y_R = H_t/G_o$

where:

H_t = total horizontal irradiance for an array plane (Wh/m^2)

and G_o = global irradiance for STC (W/m^2).

Final yield.

Final yield, which is represented as units of kW h/d∗kWp, refers to a system's daily, monthly or yearly net AC power production divided by peak energy capacity for a PV array. This is formulated for STC at 25 °C for each cell temperature and 1000 W/m^2 of solar irradiance.

$Y_F = E_{PV,\ AC}/P_{max\ G,\ STC}$.

Performance ratio.

Dividing the final yield by the reference yield gives the performance ratio. In our case, it compares the energy facility's output with potential output that considers the impact of factors such as irradiation irregularities, grid availability, aperture size, temperatures of PV panels, etc. $PR = Y_F/Y_R$.

Capacity utilization factor.

This factor represents the actual maximum power output of an energy-producing facility in comparison to its potential (or theoretical) maximum output.

CUF = Energy measured (kWh) / (365 ∗ 24 ∗ installed capacity of the plant).

Inverter efficiency.

Also known as "conversion efficiency", inverter efficiency represents the ratio of AC energy produced in an inverter to DC energy produced in a PV array system. Inverter efficiency is formulated as:

$\eta_{inv} = P_{AC}/P_{DC}$.

System efficiency.

System efficiency (as a daily measurement) is represented by PV module efficiency times inverter efficiency and is written as:

$\eta sys,_T = \eta_{PV,T} * \eta inv,_T$.

Power generated and directed to grid.

Power output in a PV system indicates the 60-second total amount of power streaming through inverter terminals and is represented by AC power production for either daily or monthly amounts.

2.2. Power loss.

These losses occur under various kinds of operational conditions and are distributed across several different parts of a grid connected SPV energy producer under real operating conditions. They are recorded through standard data collection. The main types of power losses are array capture losses and system losses.

Array capture loss (L_C) (thermal capture loss and other kinds of capture loss).

Thermal capture losses (L_{CT}): These losses can occur if cell temperatures exceed 25 °C and represent the difference between corrected and standard reference fields.

Other (miscellaneous) capture losses (L_{CM}): These losses can occur due any number of different situations and factors, including errors in maximum power tracking, partial shadowing or low irradiance, mismatching, and string diode and wiring issues. $L_{CT} = Y_R - Y_{CR}$.

$L_{CM} = Y_{CR} - Y_A$

$L_C = Y_R - Y_A$.

System losses (L_S).

System losses can be due to issues such as faulty passive circuit elements, conduction, or inverters.

$L_S = Y_A - Y_F$.

2.3. PVSYST software.

The present study uses PVSYST software [32] to conduct simulations and gauge the proposed solar energy facility's performance under different conditions and for a variety of parameters and measures. In general, PVSYST enables the importation of both personnel and meteo data and can use refined module selection to gauge system performance for a range of systems (e.g., pumping, stand-alone, grid-connected, etc.). It can also estimate yields through applying data derived from simulations. PVSYST is applied here for estimating yearly power outputs for the 10 MW peak grid-connected solar PV energy facility in PEI.

3. PVSYST simulations and results.

The power added to the grid annually is 12,185 MW h., with the maximum amount of power being produced in the Northern Hemisphere summer month July (1,293 MW h) and the minimum amount in the Northern Hemisphere fall/winter month December (495 MW h). (See Table1).

Table 1. Balances and main results.

Months	GlobHor kWh/m2	DiffHor kWh/m2	T Amb °C	Globlnc kWh/m^2	GlobEff kWh/m^2	EArray MWh	E-Grid MWh	PR
January	41.5	23.00	-7.02	77.5	75.8	766	748	0.966
February	56.8	31.80	-6.82	85.5	83.4	831	813	0.951
March	99.3	46.90	-2.62	129.0	125.8	1227	1201	0.931
April	126.7	65.60	3.15	132.4	128.3	1219	1194	0.901
May	156.4	80.30	9.20	141.8	136.8	1273	1247	0.879
June	172.6	81.80	14.73	148.7	143.3	1284	1257	0.845
July	175.2	80.10	19.18	155.9	150.4	1320	1293	0.829
August	156.5	74.60	18.82	155.2	150.2	1314	1288	0.830
September	115.0	49.30	14.74	138.1	134.3	1188	1165	0.843
October	70.8	35.90	9.48	101.9	99.4	917	897	0.881
November	38.5	23.70	4.04	63.7	62.2	601	586	0.919
December	28.0	17.50	-2.48	52.5	51.3	510	495	0.943
Year	1237.3	610.50	6.27	1382.2	1341.2	12450	12185	0.881

Where:

GlobHor: horizontal global irradiation. DiffHor: Horizontal diffuse irradiation.

T Amb: ambient temperature. GlobInc: global incident in coll. Plane.

GlobEff: effective global irradiance. EArray: effective energy at the output of the array.

E-Grid: energy injected in to grid. PR: performance ratio (%).

Primary output.

As shown in Table 1, the total power derived from the PV array measures 12,450 kW h annually.

3.1 Performance ratio.

The mean yearly performance ratio has been estimated at 88.1%.

3.2 Standard output.

LC value: 0.38 kWh/kW p/day

LS value: 0.07 kWh/kW p/day

YF: 3.34 kWh/kW p/day (Figure. 1).

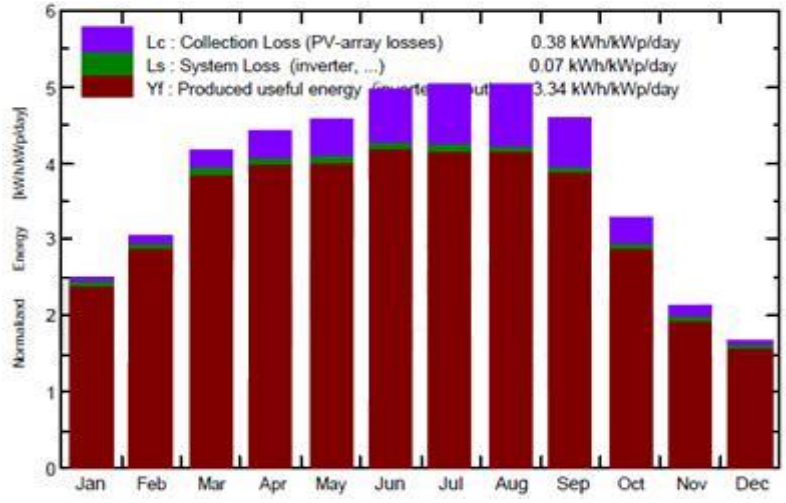

Fig. 1. Normalized energy per month

3.3 Loss diagram.

Since global horizontal irradiance measures 1,237 kWh/m^2 and the collector plane's effective irradiation measures 1,341 kWh/m^2, there is an approximate 3% power loss. When solar panel solar energy incident changes into electrical power, we have a nominal array power measure of 13,623 MWh, following PV conversion. STC readings show a PV array efficiency of just over 11%, so the array energy simulation measures 12,450 MWh, which then drops to 12,185 MWh at the inverter output when factoring in inverter losses of available power, as shown in Figure. 2 [4].

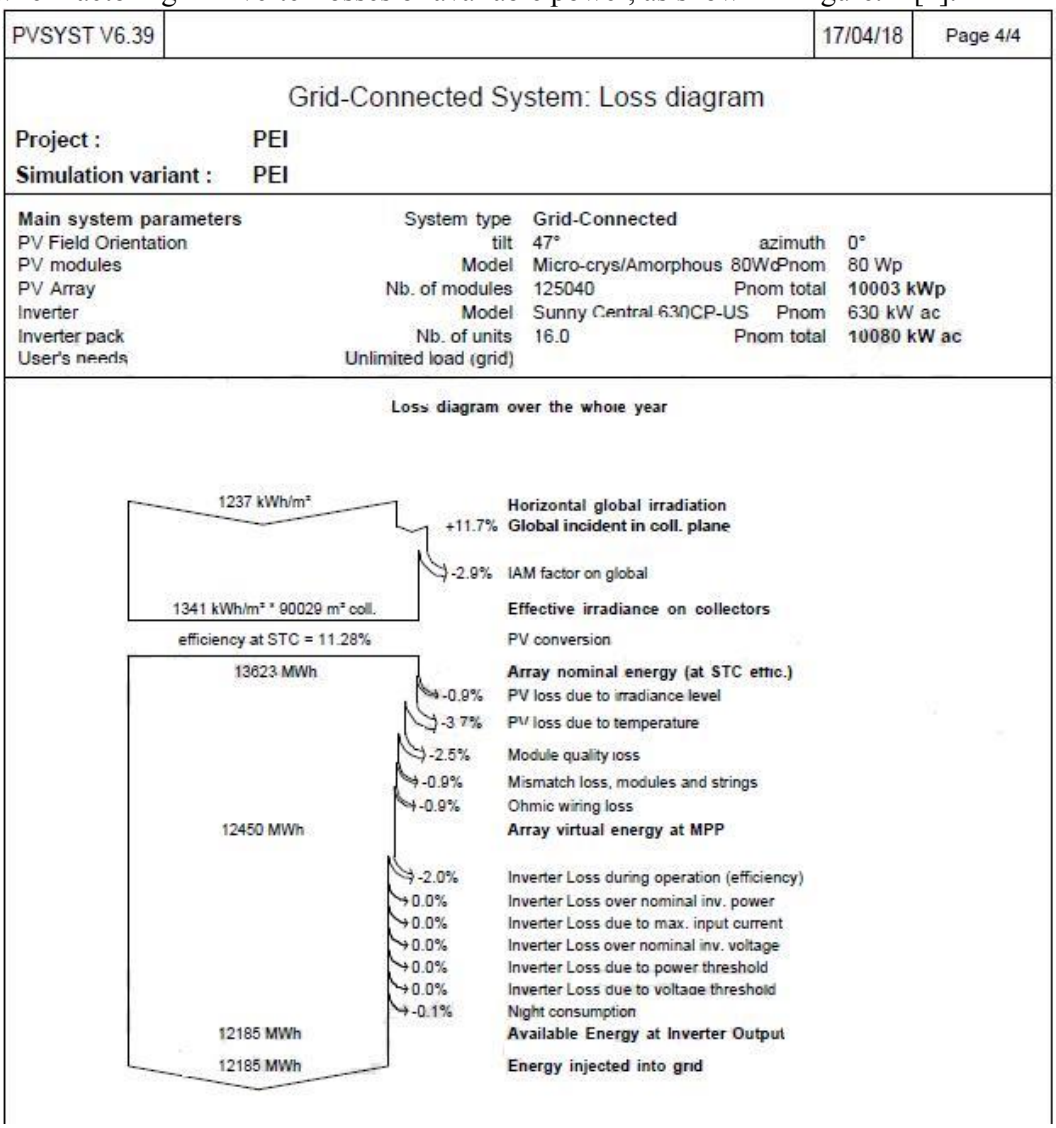

Fig. 2. Loss diagram over the entire year.

B. Wind R&D Park grid.

Situated in blustery North Cape in the Prince Edward Island province (PEI), the Wind Energy Institute of Canada has a 204 MW installed wind capacity and a 260 MW peak load. It also has a 2 MWh BESS and a 10 MW wind R&D facility. PEI and the neighboring province of New Brunswick (NB) connect via a cable of 200 MW; however, conditions of high load or light winds breach the limit, requiring diesel generators to be employed to satisfy energy demands on PEI.

Recently, under light wind conditions, the Institute employed the 2 MWh BESS for offsetting power usage in the 10 MW wind R&D facility. Specifically, they had charged their BESS in high wind conditions and then fed the stored power into the network via turbines if wind power measured under 0 kW. Such application of the BESS enables wind-derived energy to be used in a variety of circumstances, with the aim of improving efficiency and lowering costs [28].

Wind R&D facility. The Institute's wind R&D facility houses 5 turbines (DE Wind 9.2 model), each with a rotor of 93 m in diameter and rated at 2MW for output. The turbines feature synchronous generators attached at variable speed shafts via hydraulic Voiture Winder. The 1 MW-2 MWh BESS located in this facility is an S&C Pure Wave inverter system that interfaces General Electric Durathon batteries. The site also features a diesel generator to be used as a back-up to substation energy in case of lengthy transmission network outages. The 5 turbines and BESS connect via different SCADA systems as Figure 3.

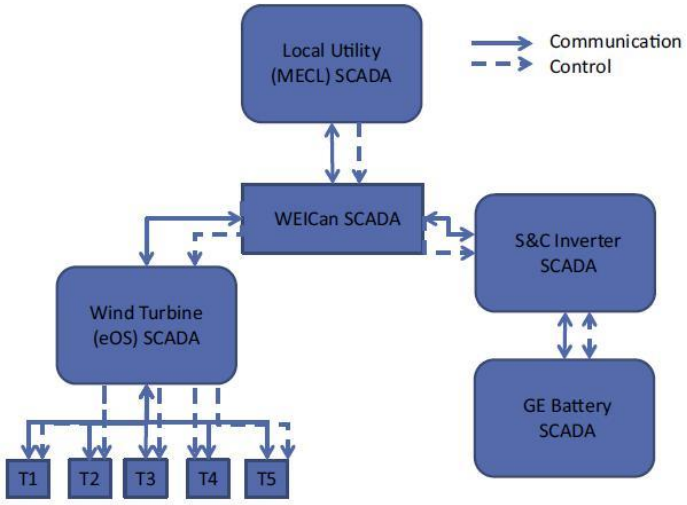

Fig. 3. WEICan SCADA's and the interaction between them.

Figure. 4. shows a sketch of the Institute's BESS in the wind facility. The facility employs automated generation control (second by second) to balance demand and power supply and ensure that the frequency is maintained at between 50 and 60 Hz. BESS has been shown to help regulate this process by storing energy at peak wind times and releasing it when winds are light, or demand is high [28].

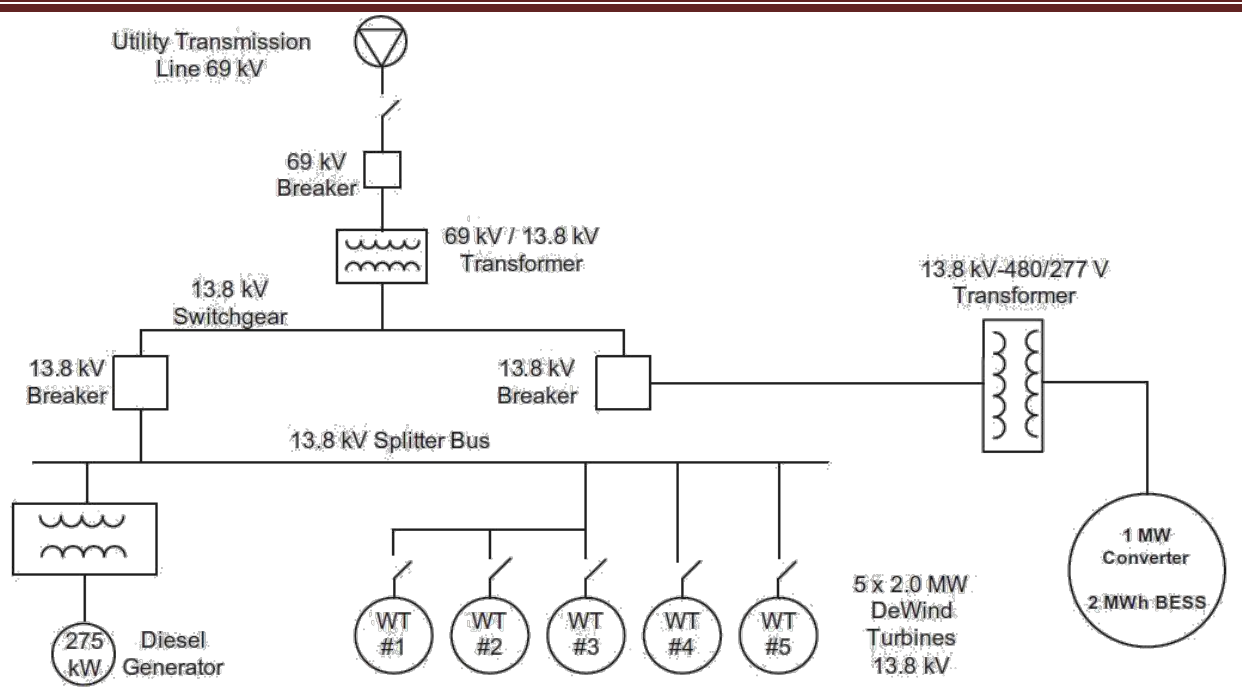

Fig. 4. Single line diagram of WEICan's Wind R&D Park.

C. Modeling of BESS.

Storage batteries in power systems obtain electrical power through the form of a direct current, which they then convert and store as energy via electrochemical changes. Nowadays, fluctuations which occur during the generation of solar or wind energy can be resolved or "smoothed" through the use of a battery energy storage station (BESS) system. These kinds of hybrid energy production systems need a reliable control method which is able to moderate a battery's state of charge (SOC) as well as the power output [33]. The present work outlines the main outcomes of a simulation analysis for a wind/PV (photovoltaic)/BESS hybrid power system that looked at various approaches to enhancing the smoothing effects for the system. The work also investigates the performance parameters for an SOC battery control. In the study, we modeled a 100-kWh lithium iron phosphate (LiFePO4) lithium-ion BESS based on the approach adopted in [34]-[35]. Figure 5 illustrates a Thevenin-equivalent battery circuit model [36].

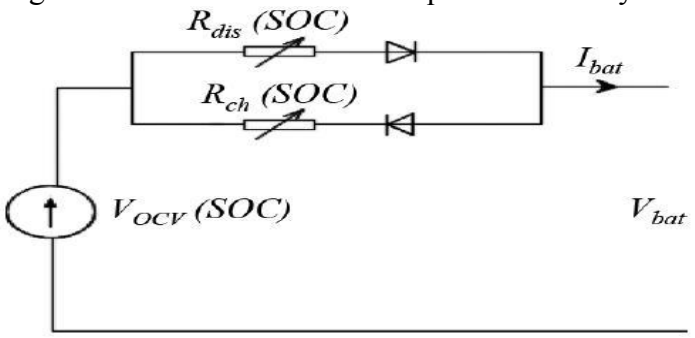

Fig. 5. Thevenin equivalent battery model.

Figure. 6. illustrates various features of open circuit voltage in a battery SOC, while Figure. 7. illustrates internal resistance.

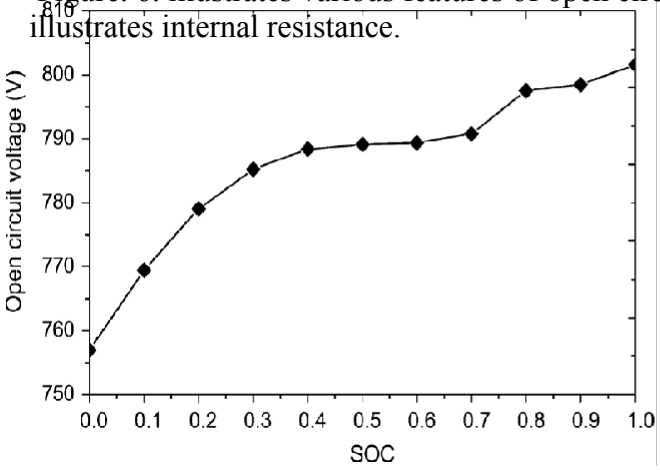

Fig. 6. Characteristic of open circuit voltage via battery SOC

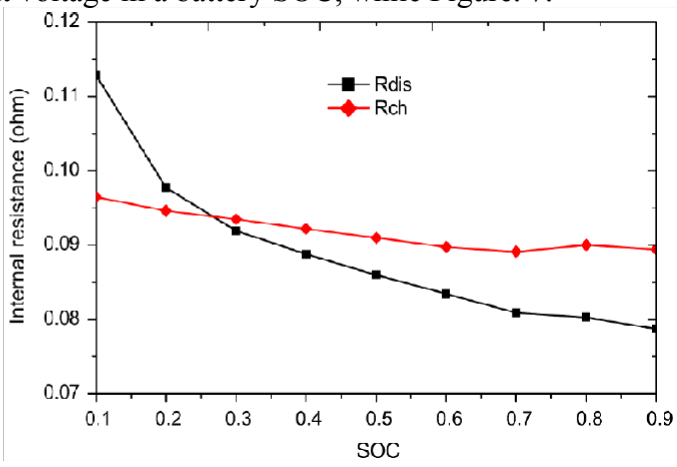

Fig. 7. Internal resistance via battery SOC

Equations (1) to (5) are applied to formulate a battery SOC according to the status of the battery charge and discharge.

$$V_{bat} = V_{ocv} - R_{bat}^{int} * I_{bat} \quad (1)$$

$$V_{ocv} = f_1(SOC) \quad (2)$$

$$R_{bat}^{int} = \{R_{ch} = f_2(SOC)\ Charging\}, OR\ \{R_{dis} = f_3(SOC)\ Discharging\}. \quad (3)$$

$$SOC = SOC_{ini} - \frac{\int \eta I_{bat}}{Q_{bat} dt} \quad (4)$$

$$\eta = \left\{\eta_{ch} = \frac{V_{ocv}}{V_{ocv} - I_{bat} * R_{ch}}\ Charging\right\}, OR\ \left\{\eta_{dis} = \frac{V_{ocv} - I_{bat} * R_{dis}}{V_{ocv}}\ Discharging\right\} \quad (5)$$

Where,

V_{bat}: Terminal voltage of battery energy storage system (V).
I_{bat}: Current of battery energy storage system (A).
V_{ocv}: Open circuit voltage of battery (V).
R_{bat}^{int}: Internal resistance of battery energy storage system (Ω).
R_{ch}: Internal resistance of charge (Ω).
R_{dis}: Internal resistance of discharge (Ω).
SOC: State of charge (%).
SOC_{ini}: Initial value of SOC (%).
η : Charging/discharging efficiency (%).
η_{ch}: Efficiency of charge (%).
η_{dis}: Efficiency of discharge (%).
Q_{bat}: Battery energy storage system capacity (kWh).

As can be seen, the symbol "- "is used to refer to BESS charging power and "+" indicates BESS discharging power. Here, we use a 2-MWh BESS formed through the integration of ten 200-kWh LiFePO4 lithium-ion BESS systems set parallel to each other. Table 2 shows the details for the 2-MWh BESS [37].

Table 2. SPECIFICATION OF BATTERY ENERGY STORAGE SYSTEM

Index	Description
Whole system	Ten 200kWh BESS in Parallel
Every 200kWh BESS	Two 100kWh BESS in Parallel
Every 100kWh BESS	Ten Battery Modules in Series

1 Module	24 - 120Ah single batteries in series
Single Battery Capacity	120Ah-(two 60Ah batteries in parallel)
Rated Power	5 x 200kWh = 2MWh
Maximum Working Voltage	840V
Minimum Working Voltage	696 V

SIMULATION and ANALYSIS.

Several different data sources were consulted to construct the model and run the simulation. The data assisted in the analysis of the hybrid system's active and reactive power variations. Applying a range of parameters resultedin the variations depicted in Figures. For connecting the grid, a combination wind turbine-PV-battery-based hybrid energy-production system was developed, and a simulation run using an enhanced P&O approach in relation to the MPPT for PV/WT [33]. MATLAB/SIMULINK software was used for verifying the system while simulation analyses were done on a Wind Farm/PV/BESS/DG hybrid model which integrated BESS systems of 10 MW WT, 10 MW PV, 1MW-2MWh BESS, and 275 kW Diesel Generator. By using a point of common coupling, the BESS, WT, PV, and Diesel Generator were connected to a utility-grid energy system. Figure. 8. Illustrates the system. As can be seen, it comprises several different elements or energy-production blocks, including measurement, inverter and grid utility blocks, wind turbines, PV, batteries, converter and electrical parameters.

In the simulations, the battery SOC adjustable range was set between 10% and 90% [37]. It is worth mentioning here that the output of renewable energies relies heavily on data representi

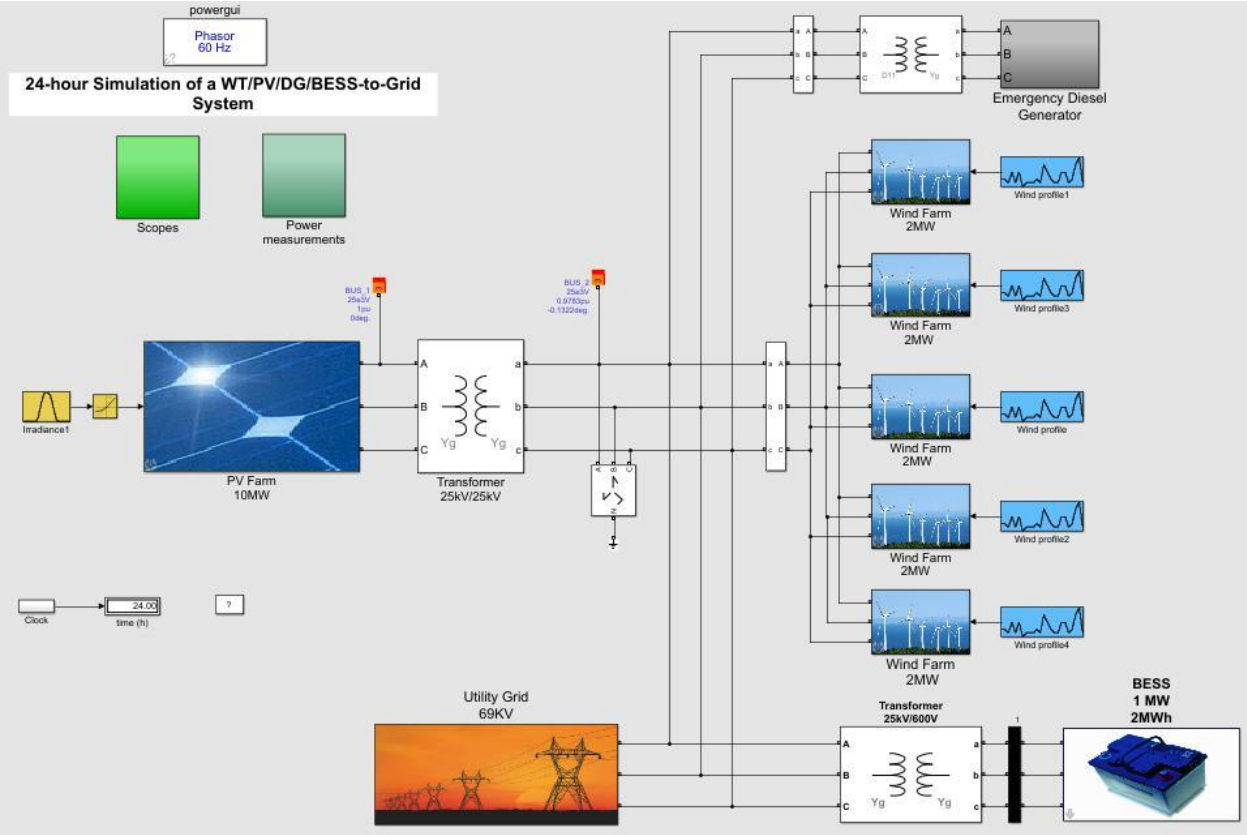

Fig. 8. SIMULINK Model of Hybrid Power System

signals that change over time by employing a signal builder. Using data for a certain locale, solar irradiance and wind speed are recorded using the simulation lasts 24 hours. Overall, the simulation ran for 24 hours in total. The solar intensity follows a normal distribution where the highest intensity is reached at midday. The wind varies greatly during the day and has multiple peaks and lows. the circuit was tested during a low day in wind speed at July 14 for 24 hours to show the charging and discharging of BESS. Figure 9 depicts wind turbine outcomes, Figure. 10. depicts PV outcomes, and Figures. 11, 12 and 13 depict charge, discharge, and SOC of BESS, respectively.

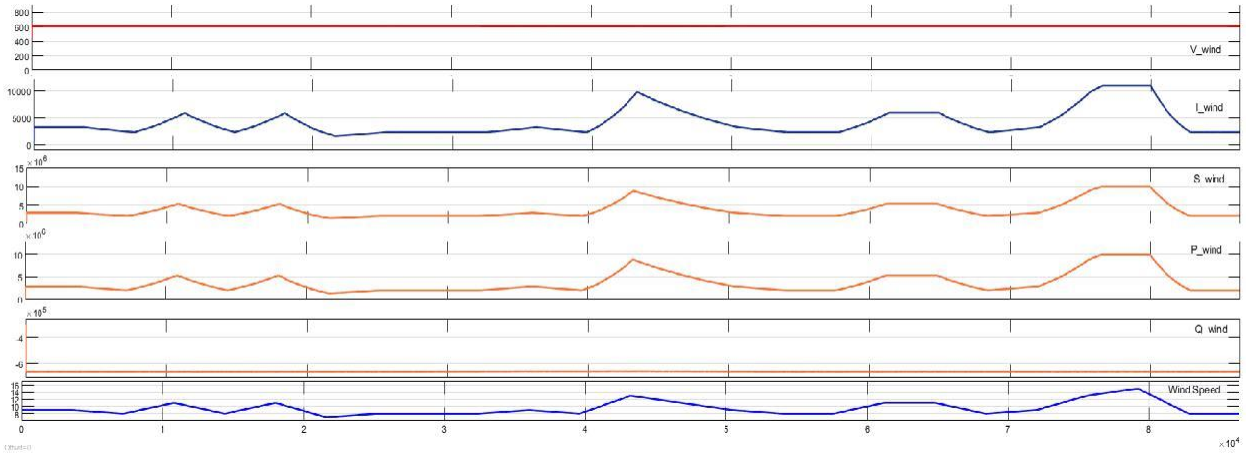

Fig. 9. Simulation of 24-hours to Wind Turbines.

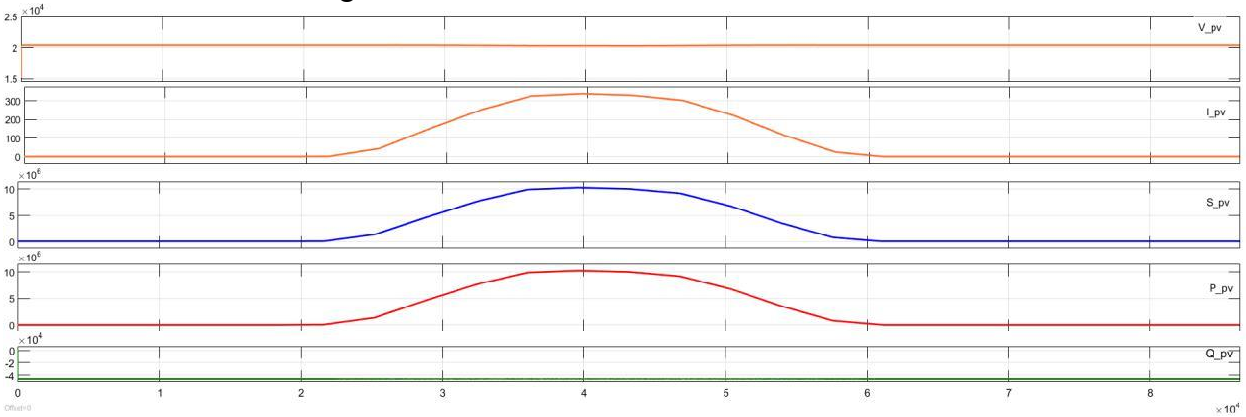

Fig. 10. Simulation of 24-hours to PV.

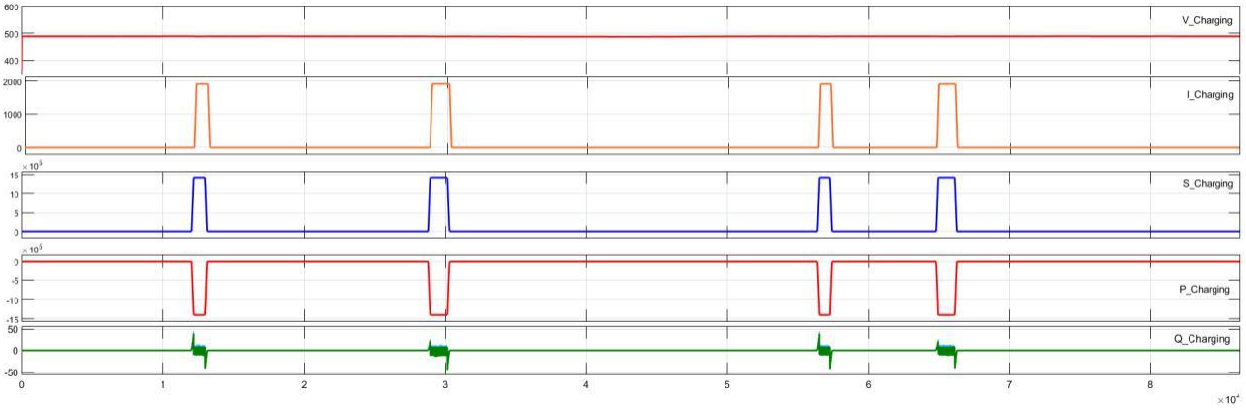

Fig. 11. Simulation of 24-hours to Charging of BESS.

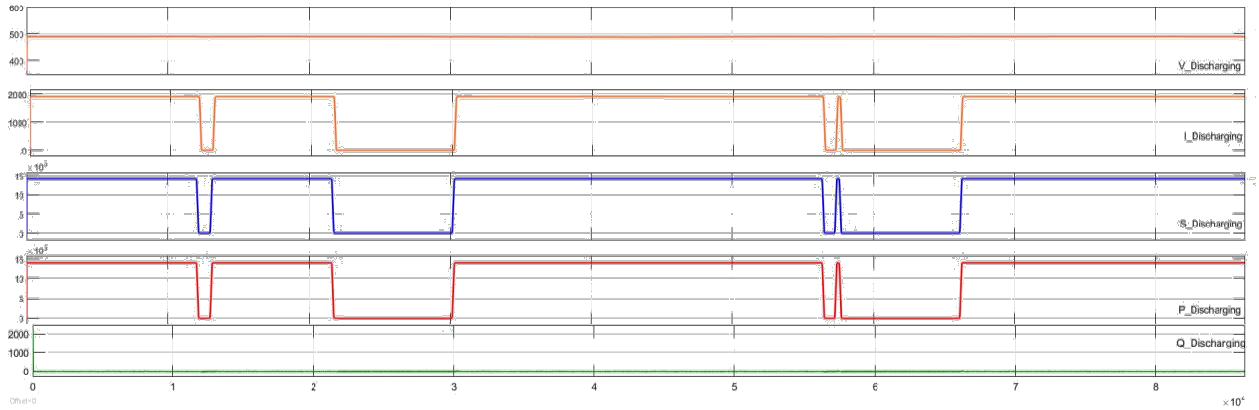

Fig. 12. Simulation of 24-hours to Discharging of BESS.

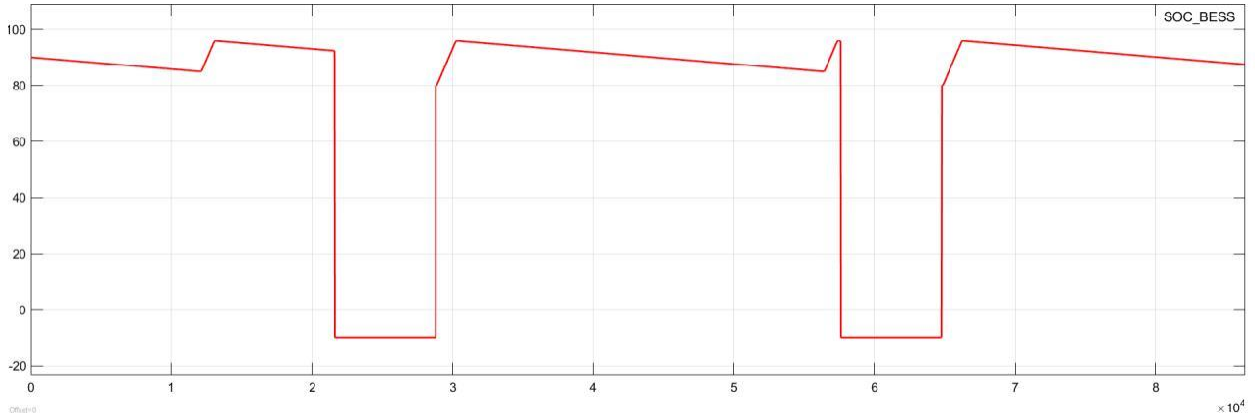

Fig. 13. Simulation of 24-hours to SOC of BESS.

Figures 14, 15 indicate the amount of energy being produced by both PV and WT for two separate cases: Case 1 represents power produced by PV and WT; Case 2 represents power produced by PV, WT, and charging and discharging a battery, respectively.

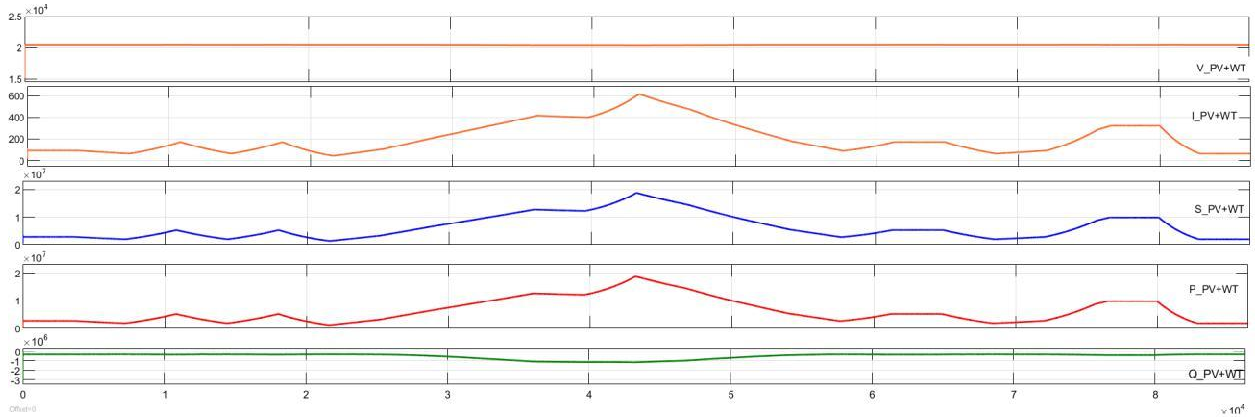

Fig Simulation of 24-hours to power produced by PV and WT. 14..

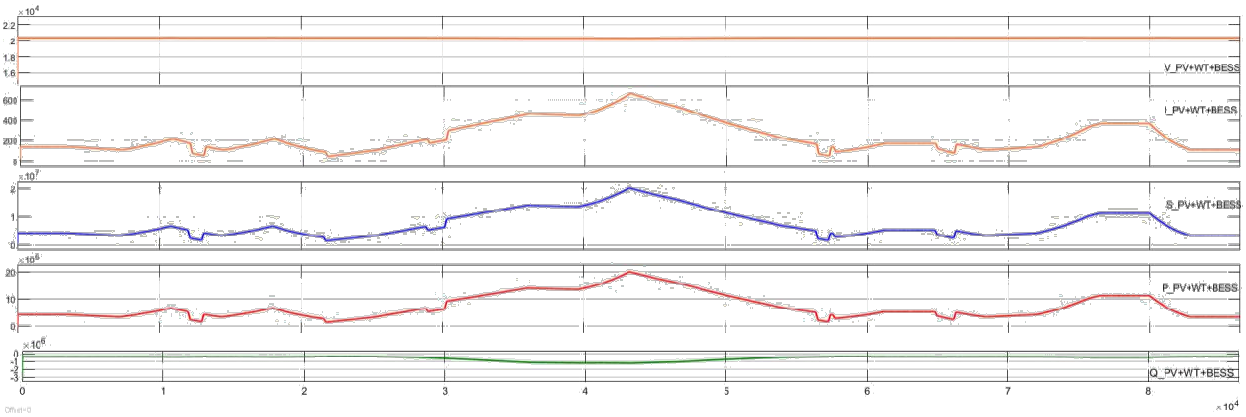

Fig. 15. Simulation of 24-hours to power produced by PV, WT, and BESS.

Summary and Conclusion.

This work presented a performance study on modeling a 10-MW peak grid-connected solar PV power-production plant intended for installation on Prince Edward Island, Canada. The plant would be evaluated every year. The aim was to connect the PVs to wind turbines that are already in service in order to double the existing 10 MW of power generation to 20 MW. To accomplish the simulated integration, MATLAB SIMULINK software was employed for testing the proposed system according to a range of operational parameters. Also, in the simulation, we used a BESS connected to the hybrid system as a means to decrease power fluctuations and enhance system stability, and differences in charging/discharging of the battery were investigated. Future potential related research includes designing an energy management system (EMS) for integrating energy produced by different types of sources to feed loads and contribute to smoothing during BESS charge/discharge cases.

References.

[1] Makrides, G., Zinsser, B., Norton, M., Georghiou, G.E., Schubert, M., Werner, J.H., 2010. "Potential of photovoltaic systems in Countries with high solar irradiation". Renewable Sustainable Energy Rev. 14, 754–762.

[2] Besarati, S.M., Padilla, R.V., Goswami, D.Y., Stefanakos, E., 2013. "The potential of harnessing solar radiation in Iran: generating solar maps and viability study of PV power plants". Renew Energy 53, 193–199.

[3] Elhodeiby, A.S., Metwally, H.M.B., Farahat, M.A., 2011. "Performance analysis of 3.6 kW Rooftop grid connected photovoltaic system in Egypt". International Conference on Energy Systems and Technologies, Cairo, Egypt, CEST 2011, 11–14 March.

[4] B. Shiva Kumar, K. Sudhakar,2015. "Performance evaluation of 10 MW grid connected solar photovoltaic power plant in India". Energy Reports 1 (2015) 184–192.

[5] Council GWE. Global wind report – annual market update 2013. Belgium; 2014.

[6] Half-Year Report 2014 [press release]. Germany; September 17, 2014.

[7] Zhao H, Wu Q, Hu S, Xu H, Rasmussen CN. "Review of energy storage system for wind power integration support". Appl Energy 2015,545–53.

[8] Zafirakis D, Chalvatzis KJ, Baiocchi G, Daskalakis G. "Modeling of financial incentives for investments in energy storage systems that promote the largescale integration of wind energy". Appl Energy 2013; 105:138–54.

[9] Wu Guohong, Yoshida Yutaka, Minakawa Tamotsu. "Grid-connected Wind Park with combined use of battery and EDLC energy storages". INTECH; 2012.

[10]

[10] Baccino F, Grillo S, Marinelli M, Massucco S, Silvestro F, Baccino F, et al. “Power and energy control strategies for a Vanadium Redox Flow Battery and wind farm combined system”. 2nd IEEE PES international conference and exhibition on innovative smart grid technologies. IEEE; 2011.
[11] Grillo Samuele, Marinelli Mattia, Massucco Stefano, Silvestro Federico, Di Rosa Daniela, Fastelli Irene, Gigliucci Gianluca. “Generation and battery modelling and integrated control strategies for a better acceptance of intermittent renewable energy sources in the electric distribution system”. CIRED; Lyon 2010.
[12] Spahic E, Balzer G, Shakib AD, editors. “The impact of the ‘‘wind farm – battery’’ unit on the power system stability and control”. Power Tech, 2007 IEEE Lausanne, 2007; 1–5 July 2007.
[13] Borhan H, Rotea MA, Viassolo D, editors. “Control of battery storage for wind energy systems”. American Control Conference (ACC), 2012; 27–29 June 2012.
[14] Jansen Ryan, Sulatisky Micheal, Farber Anton, Muyres Dallan. “Demonstration of a utility-scale lithium-ion battery system with a wind turbine”. Electrical energy storage applications and technologies conference; 2013.
[15] Alliance CES. “Energy storage – a cheaper, faster, & cleaner alternative to conventional frequency regulation”. Berkeley, CA; 2011.
[16] Huajie D, Zechun H, Yonghua S, Jincheng W, Xiaoxu F, editors.” Coordinated operational strategy of energy storage system and wind farm. Innovative smart grid technologies Europe (ISGT EUROPE)”, 2013 4th IEEE/PES; 2013, 6–9 Oct. 2013.
[17] H. Yang, Z. Wei, and L. Chengzh, “Optimal design and technoeconomic analysis of a hybrid solar-wind power generation system,” Applied Energy, vol. 86, pp. 163-169, Feb. 2009.
[18] S. Dihrab, and K. Sopian, “Electricity generation of hybrid PV/wind systems in Iraq,” Renewable Energy, vol. 35, pp. 1303-1307, Jun.2010.
[19] J.P. Reichling, and F.A. Kulacki, “Utility scale hybrid wind-solar thermal electrical generation: a case study for Minnesota,” Energy, vol. 33, pp.626-638, Apr. 2008.
[20] O. Ekren, B.Y. Ekren, and B. Ozerdem, “Break-even analysis and size optimization of a PV/wind hybrid energy conversion system with battery storage – A case study” Applied Energy, vol.86, pp. 1043-1054, July-August 2009.
[21] S.K. Kim, J.H. Jeon, C.H. Cho, E.S. Kim, and J.B. Ahn, “Modeling and simulation of a grid-connected PV generation system for electromagnetic transient analysis,” Solar Energy, vol.83, pp. 664-678, May 2009.
[22] H.L Tsai, “Insolation-oriented model of photovoltaic module using Matlab/Simulink,” Solar Energy, vol. 84, pp. 1318-1326, July 2010.
[23] Adriana Luna, Nelson Diaz, Mehdi Savaghebi, Juan C. Vasquez, Josep M. Guerrero,” Optimal Power Scheduling for a Grid-Connected Hybrid PV-Wind-Battery Microgrid System”, IEEE,2016.
[24] M.J. Khan, and M.T. Iqbal, “Dynamic modeling and simulation of a small wind fuel cell hybrid energy system,” Renewable Energy, vol. 30, pp. 421-439, Mar. 2005.
[25] N. Chayawatto, K. Kirtikara, V. Monyakul, C. Jivacate, and D. Chenvidhya, “DC–AC switching converter modelings of a PV grid-connected system under islanding phenomena,” Renewable Energy, vol. 34, pp. 2536-2544, Dec. 2009.
[26] Lihui Zhang, He Xin, Jing Wu, Liwei Ju, and Zhongfu Tan,” A Multiobjective Robust Scheduling Optimization Mode for Multienergy Hybrid System Integrated by Wind Power, Solar Photovoltaic Power, and Pumped Storage Power”, Hindawi Journal, Mathematical Problems in Engineering, 2017, Article ID 9485127, 15 pages.
[27] E. M. Natsheh, A. Albarbar, J. Yazdani,” Modeling and control for smart grid integration of solar/wind energy conversion system” ,2011 ,2nd IEEE PES International Conference and Exhibition on Innovative Smart Grid.
[28] David Watson, Tapabrata Chakraborty, Marianne Rodgers,” The need for SCADA communication in a Wind R&D Park”, Sustainable Energy Technologies and Assessments,2015,65–70.
[29]

[30] Green Infra Solar Energy Limited,"10 MW Solar Photovoltaic Power Plant in Rajkot, Gujarat (India)", 2012.
[31] Baccino F, Grillo S, Marinelli M, Massucco S, Silvestro F, Baccino F, et al. "Power and energy control strategies for a Vanadium Redox Flow Battery and wind farm combined system". 2nd IEEE PES international conference and exhibition on innovative smart grid technologies. IEEE; 2011.
[32] Grillo Samuele, Marinelli Mattia, Massucco Stefano, Silvestro Federico, Di Rosa Daniela, Fastelli Irene, Gigliucci Gianluca. "Generation and battery modelling and integrated control strategies for a better acceptance of intermittent renewable energy sources in the electric distribution system". CIRED; Lyon 2010.
[33] Spahic E, Balzer G, Shakib AD, editors. "The impact of the ''wind farm – battery'' unit on the power system stability and control". Power Tech, 2007 IEEE Lausanne, 2007; 1–5 July 2007.
[34] Borhan H, Rotea MA, Viassolo D, editors. "Control of battery storage for wind energy systems". American Control Conference (ACC), 2012; 27–29 June 2012.
[35] Jansen Ryan, Sulatisky Micheal, Farber Anton, Muyres Dallan. "Demonstration of a utility-scale lithium-ion battery system with a wind turbine". Electrical energy storage applications and technologies conference; 2013.
[36] Alliance CES. "Energy storage – a cheaper, faster, & cleaner alternative to conventional frequency regulation". Berkeley, CA; 2011.
[37] Huajie D, Zechun H, Yonghua S, Jincheng W, Xiaoxu F, editors." Coordinated operational strategy of energy storage system and wind farm. Innovative smart grid technologies Europe (ISGT EUROPE)", 2013 4th IEEE/PES; 2013, 6–9 Oct. 2013.
[38] H. Yang, Z. Wei, and L. Chengzh, "Optimal design and technoeconomic analysis of a hybrid solar-wind power generation system," Applied Energy, vol. 86, pp. 163-169, Feb. 2009.
[39] S. Dihrab, and K. Sopian, "Electricity generation of hybrid PV/wind systems in Iraq," Renewable Energy, vol. 35, pp. 1303-1307, Jun.2010.
[40] J.P. Reichling, and F.A. Kulacki, "Utility scale hybrid wind-solar thermal electrical generation: a case study for Minnesota," Energy, vol. 33, pp.626-638, Apr. 2008.
[41] O. Ekren, B.Y. Ekren, and B. Ozerdem, "Break-even analysis and size optimization of a PV/wind hybrid energy conversion system with battery storage – A case study" Applied Energy, vol.86, pp. 1043-1054, July-August 2009.
[42] S.K. Kim, J.H. Jeon, C.H. Cho, E.S. Kim, and J.B. Ahn, "Modeling and simulation of a grid-connected PV generation system for electromagnetic transient analysis," Solar Energy, vol.83, pp. 664-678, May 2009.
[43] H.L Tsai, "Insolation-oriented model of photovoltaic module using Matlab/Simulink," Solar Energy, vol. 84, pp. 1318-1326, July 2010.
[44] Adriana Luna, Nelson Diaz, Mehdi Savaghebi, Juan C. Vasquez, Josep M. Guerrero," Optimal Power Scheduling for a Grid-Connected Hybrid PV-Wind-Battery Microgrid System", IEEE,2016.
[45] M.J. Khan, and M.T. Iqbal, "Dynamic modeling and simulation of a small wind fuel cell hybrid energy system," Renewable Energy, vol. 30, pp. 421-439, Mar. 2005.
[46] N. Chayawatto, K. Kirtikara, V. Monyakul, C. Jivacate, and D. Chenvidhya, "DC–AC switching converter modelings of a PV grid-connected system under islanding phenomena," Renewable Energy, vol. 34, pp. 2536-2544, Dec. 2009.
[47] Lihui Zhang, He Xin, Jing Wu, Liwei Ju, and Zhongfu Tan," A Multiobjective Robust Scheduling Optimization Mode for Multienergy Hybrid System Integrated by Wind Power, Solar Photovoltaic Power, and Pumped Storage Power", Hindawi Journal, Mathematical Problems in Engineering, 2017, Article ID 9485127, 15 pages.
[48] E. M. Natsheh, A. Albarbar, J. Yazdani," Modeling and control for smart grid integration of solar/wind energy conversion system" ,2011 ,2nd IEEE PES International Conference and Exhibition on Innovative Smart Grid.
[49] David Watson, Tapabrata Chakraborty, Marianne Rodgers," The need for SCADA communication in a Wind R&D Park", Sustainable Energy Technologies and Assessments,2015,65–70.

[50] Green Infra Solar Energy Limited,"10 MW Solar Photovoltaic Power Plant in Rajkot, Gujarat (India)", 2012.